Korea-Australia Rheology Journal
Vol. 14, No. 3, September 2002 pp. 107-114

Measurement of residual stresses in injection molded short fiber composites considering anisotropy and modulus variation

Sang Kyun Kim[1], Seok Won Lee and Jae Ryoun Youn*
School of Materials Science and Engineering, Seoul National University, Seoul 151-742, Korea
[1]KOLON Central Research Institute, Kyungki-do, Korea

(Received July 25, 2002)

Abstract

Residual stress distribution in injection molded short fiber composites is determined by using the layer-removal method. Polystyrene is mixed with carbon fibers of 3% volume fraction (4.5% weight fraction) in an extruder and the tensile specimen is injection-molded. The layer-removal process, in which removing successive thin uniform layers of the material from the surface of the specimen by a milling machine, is employed and the resulting curvature is acquired by means of an image processing. The isotropic elastic analysis proposed by Treuting and Read which assumes a constant Young's modulus in the thickness direction is one of the most frequently used methods to determine residual stresses. However, injection molded short fiber composites experience complex fiber orientation during molding and variation of Young's modulus distribution occurs in the specimen. In this study, variation of Young's modulus with respect to the thickness direction is considered for calculation of the residual stresses as proposed by White and the result is compared with that by assuming constant modulus. Residual stress distribution obtained from this study shows a typical stress profile of injection-molded products as reported in many literatures. Young's modulus distribution is predicted by using numerical methods instead of experimental results. For the numerical analysis of injection molding process, a hybrid FEM/FDM method is used in order to predict velocity, temperature field, fiber orientation, and resulting mechanical properties of the specimen at the end of molding.

Keywords : residual stress, injection molding, short fiber composites, layer-removal method, curvature, Young's modulus distribution

1. Introduction

Short fiber reinforced composites are getting widely used in the technical and industrial applications due to good mechanical properties. They are usually manufactured by injection molding, compression molding, resin transfer molding, and extrusion. Among these processes, injection molding is the most important commercial process because of the easiness of manufacture and economical advantages. During injection molding process of composites, a complex resin flow field is generated and it causes fibers to be oriented. The orientation of fibers will be changing until the matrix is solidified.

Due to the high pressure gradient, temperature change caused by inhomogeneous cooling of the polymer melt, orientation of polymer chains and the difference in thermal expansion coefficient between matrix and fibers, residual stresses may be introduced in the materials. These residual stresses result in warpage and shrinkage of the final products and may induce reduction of tensile strength, fatigue strength, impact properties, and environmental stress cracking. Thus, the dimensional accuracy and properties of the final products are highly related to the residual stress distribution in the molded part. In order to obtain a desired injection molded composite, it is important to understand internal stress development along with the molding procedure and to measure the residual stress distribution in molded composite materials.

Layer-removal method has been the primary method used to measure the residual stress in polymeric materials. Residual stresses can be measured by the layer-removal method proposed by Treuting and Read (1951). In the analysis, thin layers of uniform thickness are machined from the surface of the rectangular specimen, and the layer removal causes upsetting the residual stress equilibrium in the specimen. Then, the specimen warps to a shape of a circular arc to restore equilibrium. One can determine the gapwise residual stresses in the specimen before layer removal by measuring the resulting curvature as a function

*Corresponding author: jaeryoun@gong.snu.ac.kr

of removed depth. The Treuting and Read analysis is applicable to a linear elastic material with isotropic elastic constants. However, injection moldings often have a significant depth-dependent variation in stiffness, whether unfilled or filled with short-fiber reinforcement. When the Young's modulus varies with depth, the simplifications made by Treuting and Read are no longer valid and it has been pointed out that this may lead to errors in the unmodified Treuting and Read analysis (White, 1985). Paterson and White (1989) proposed a procedure in which the residual stress distribution of polymeric materials with depth-varying Young's modulus could be determined. Injection-molded neat nylon 66 bars treated in different conditions were used so that they had different gapwise Youngs modulus profiles. It was shown that the residual stress distribution could be determined as long as the modulus distribution is known. The experimental procedure is the same as the layer removal method by Treuting and Read.

In this work, the residual stress distribution of injection molded short fiber reinforced composites is determined using layer removal method. To overcome the limitation of Treuting and Read analysis caused by neglecting the depth-varying Young's modulus in injection molded short fiber reinforced composites, White analysis is used and the results are compared with those of Treuting and Read analysis. For the experiment, tensile specimens are injection molded with polystyrene reinforced by 3 vol% (4.5 wt%) short carbon fibers. Young's modulus distribution through the thickness needed for White analysis is predicted numerically based on the work done by Lee and Youn (1997; 1999).

2. Theory

2.1. Layer-removal method

2.1.1. Analysis with constant modulus

The analysis applies to sheet materials and involves removing successive uniform layers from the surface of the material. When the following three conditions are satisfied, the accuracy of this method is subject only to the precision of the measurement (Treuting, 1951).

(1) To determine the stress from the curvature, it is necessary that the material be linear in pure bending over the range of curvatures involved and that the elastic constants be constant throughout the material. If these conditions are not satisfied, it is necessary to measure the bending moment required to straighten the specimen after every removal.

(2) The stress should not vary in the plane direction of the specimen but only through the thickness direction.

(3) The layer removal should not introduce additional stresses to the remaining material.

Since it is assumed that the stress distribution is constant

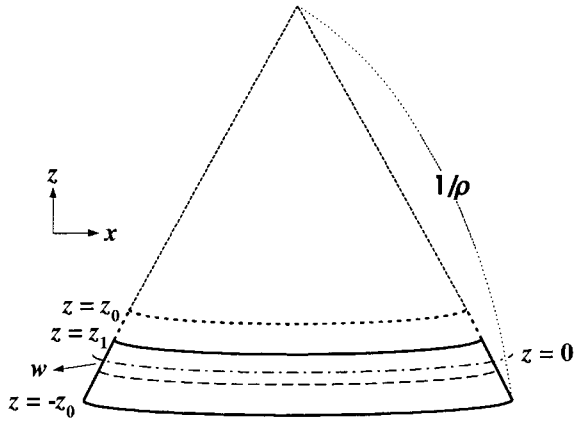

Fig. 1. Schematic diagram for determination of the curvature and coordinates.

in the x and y direction, the only remaining stress components are σ_x and σ_y. The coordinate and principal components are illustrated in Fig. 1.

Now a uniform layer is removed so that the new upper surface is at $z=z_1$. Then, the moment per unit depth about the centerline can be related with stress distribution as below.

$$M_x(z_1) = \int_{-z_0}^{z_1} \sigma_x(z)\left[z+\frac{z_0-z_1}{2}\right]dz \tag{1}$$

where M_x is moment, z_0 is half thickness, and z_1 is the thickness from the original centerline to the removed surface. For an isotropic material in the elastic range, the moment can be written as a function of resulting curvature in the x and y direction as below.

$$M_x(z_1) = \frac{-E}{12(1-\nu^2)}(z_0+z_1)^3[\rho_x(z_1)+\nu\rho_y(z_1)] \tag{2}$$

where E is modulus and ν is Poisson's ratio. ρ_x and ρ_y represent curvature in the x and y direction, respectively. Converting eq. (1) as the relation for stress and substituting eq. (2) yields the following general stress-curvature relation.

$$\sigma_x(z_1) = \frac{-E}{6(1-\nu^2)}\left[\begin{array}{l}(z_0+z_1)^2\left\{\dfrac{d\rho_x(z_1)}{dz_1}+\dfrac{\nu d\rho_y(z_1)}{dz_1}\right\}+4(z_0+z_1)\times \\ \{\rho_x(z_1)+\nu\rho_y(z_1)\}-2\int_{-z_0}^{z_1}\{\rho_x(z)+\nu\rho_y(z)\}dz\end{array}\right] \tag{3}$$

If the curvature in the transverse direction is very small, then $\rho_y=0$ and $\sigma_y=\nu\sigma_x$. Thus, eq. (3) becomes

$$\sigma_x(z_1) = \frac{-E}{6(1-\nu^2)} \times\left[(z_0+z_1)^2\frac{d\rho_x(z_1)}{dz_1}+4(z_0+z_1)\rho_x(z_1)-2\int_{-z_0}^{z_1}\rho_x(z)dz\right] \tag{4}$$

so that only the curvature in the longitudinal direction need to be measured.

2.1.2. Analysis with modulus variation

A plate is considered for the case where the Youngs modulus, $E(z)$, varies with respect to the depth, and has a residual stress distribution, $\sigma(z)$. If a uniform layer is removed so that the upper surface is located at $z=z_1$, the plate bends to restore internal force equilibrium as illustrated in Fig. 1. In the Treuting and Read analysis, the modulus is assumed to be uniform, so that the neutral surface is located at the center of the reduced plate. However, when the modulus is not uniform, the location of the neutral surface has to be determined from the relation below.

$$\int_{-z_0}^{z_1}(z+w)E_x(z)\mathrm{d}z = 0 \tag{5}$$

where w is the distance of the neutral surface from the reference surface (z=0) and $E_x(z)$ is the Youngs modulus in the x direction. Thus, from the eq. (5), the position of neutral surface with respect to the removed depth can be determined as below.

$$w(z_1) = -\frac{\int_{-z_0}^{z_1} zE_x\mathrm{d}z}{\int_{-z_0}^{z_1} E_x\mathrm{d}z} \tag{6}$$

The bending moment per unit width about the neutral surface can be written as below.

$$M_x(z_1) = \int_{-z_0}^{z_1}(z+w)\sigma_x\mathrm{d}z \tag{7}$$

Now what we require is a suitable relation between moment and curvature when the modulus varies with respect to the depth.

$$M_x(z_1) = -\int_{-z_0}^{z_1}(z+w)^2\left[\frac{\rho_x+\nu\rho_y}{1-\nu^2}\right]E_x\mathrm{d}z \tag{8}$$

As in the Treuting and Read analysis, inverting eq. (7) for the stress yields the equation below.

$$\sigma_x(z_1) = \frac{1}{(z_1+w)}\frac{\mathrm{dM}_x}{\mathrm{dz}_1} - E_x(z_1)\int_{-z_0}^{z_1}\frac{\dfrac{\mathrm{dM}_x}{\mathrm{dz}_1}}{(z_1+w)\displaystyle\int_{-z_0}^{z_1}E_x\mathrm{dz}}\mathrm{dz} \tag{9}$$

The moment derivatives in eq. (9) can be related with curvatures from eq. (8).

$$\frac{\mathrm{dM}_x}{\mathrm{dz}_1} = \frac{-\rho_x E_x}{(1-\nu^2)}(z_1+w)^2 - \frac{1}{(1-\nu^2)}\frac{\mathrm{d}\rho_x}{\mathrm{dz}_1}$$
$$\times\left(\int_{-z_0}^{z_1}z^2E_x\mathrm{dz} + 2w\int_{-z_0}^{z_1}zE_x\mathrm{dz} + w^2\int_{-z_0}^{z_1}E_x\mathrm{dz}\right) \tag{10}$$

The curvature in the transverse direction is assumed to be very small in the above equation.

2.2. Prediction of modulus distribution

Mechanical properties of injection molded short fiber composites are strongly influenced by flow-induced fiber orientation. Thus, in order to predict modulus distribution across the thickness, fiber orientation states should be known a priori. A quasi-steady state, non-isothermal, compressible, inelastic, and creeping flow of polymer melt into a thin cavity is analyzed to predict fiber orientation states. Modified Cross model and Taits state equation are adopted to consider shear-thinning behavior and compressibility of the polymer melt. Compressible version of generalized Hele-Shaw model is developed to calculate flow field during the injection molding process. Pressure and temperature fields are obtained by the control volume based FEM/FDM hybrid numerical technique.

Orientation tensors are introduced to describe three-dimensional fiber orientation due to their ability to reduce the amount of computation significantly as well as their normality and symmetry (Advani *et al.*, 1987). The second and fourth order orientation tensors are defined as below.

$$a_{ij} = \oint p_i p_j \psi(\boldsymbol{p})\mathrm{d}\boldsymbol{p} \tag{11}$$

$$a_{ijkl} = \oint p_i p_j p_k p_l \psi(\boldsymbol{p})\mathrm{d}\boldsymbol{p} \tag{12}$$

where $\boldsymbol{p}$ denotes the unit vector in the fiber direction and ψ is the orientation distribution function. Time evolution of fiber orientation can be known from the solution of the equations of orientation change for the second order orientation tensor.

$$\frac{Da_{ij}}{Dt} = -\frac{1}{2}(\omega_{ik}a_{kj} - a_{ik}\omega_{kj}) + \frac{1}{2}\lambda(\dot{\gamma}_{ik}a_{kj} + a_{ik}\dot{\gamma}_{kj} - 2\dot{\gamma}_{kl}a_{ijkl}) + 2C_I\dot{\gamma}(\delta_{ij} - 3a_{ij}) \tag{13}$$

where $\lambda = (r_e^2-1)/(r_e^2+1)$, C_I is the interaction coefficient proposed by Folgar and Tucker (1984), and r_e is the aspect ratio of the fiber. The fourth order orientation tensors appear in the above equations and should be expressed in terms of the second order tensors to avoid recurrence. For the purpose, hybrid closure approximation suggested by Advani and Tucker (1990) is applied. The above equations are solved by the fourth order Runge-Kutta method with the upwinding scheme for convective terms so that numerical stability should be insured.

Prediction of modulus distribution is carried out by defining a unit cell in which matrix surrounds a single fiber with the same volume fraction as averaged for the entire composite. The unit cell is assumed to be transversely isotropic. The Halpin-Tsai equation (1976) is adopted to predict the modulus of the unit cell.

$$\frac{M}{M_m} = \frac{1+\zeta\xi\phi_f}{1-\xi\phi_f} \tag{14}$$

where $\xi = \dfrac{(M_f/M_m)-1}{(M_f/M_m)+\zeta}$. (15)

M denotes axial modulus, E_1, transverse modulus, E_2, axial shear modulus, G_{12}, or transverse shear modulus, G_{23}. Subscripts f and m denote fiber and matrix, respectively. ϕ_f is the volume fraction of fibers. ζ is given as below.

$$\zeta_{E_1} = 2\frac{L}{D} \tag{16}$$

$$\zeta_{E_2} = 2 \tag{17}$$

$$\zeta_{G_{12}} = 1 \tag{18}$$

$$\zeta_{G_{23}} = \frac{K_m/G_m}{K_m/G_m+2} \tag{19}$$

L and D are the length and diameter of the fiber. K_m is bulk modulus and G_m is the shear modulus of the matrix. Poisson's ratio can be obtained by the rule of mixtures.

$$\nu_{12} = \nu_f\phi_f + \nu_m(1-\phi_f) \tag{20}$$

ν_{21} and ν_{23} are given by consideration of symmetry constraints as below.

$$\nu_{21} = \nu_{12}\frac{E_2}{E_1} \tag{21}$$

$$\nu_{23} = \frac{E_2}{2G_{23}} - 1 \tag{22}$$

Elastic constants obtained by the above equations have the following relationship with the components of the contracted stiffness matrix of a unit cell.

$$C_{11} = \frac{(1-\nu_{23})E_1}{1-\nu_{23}-2\nu_{12}\nu_{21}}$$

$$C_{22} = \frac{E_2}{2(1-\nu_{23}-2\nu_{12}\nu_{21})} + G_{23}$$

$$C_{44} = G_{23}$$

$$C_{66} = G_{12}$$

$$C_{12} = \frac{\nu_{21}E_1}{1-\nu_{23}-2\nu_{12}\nu_{21}}$$

$$C_{23} = \frac{E_2}{2(1-\nu_{23}-2\nu_{12}\nu_{21})} + G_{23} \tag{23}$$

To predict the mechanical properties of the composite with an arbitrary fiber orientation, orientation averaging is needed from the properties of a unit cell.

$$\langle \mathbf{M} \rangle \equiv \oint \mathbf{M}(\mathbf{p})\psi(\mathbf{p})d\mathbf{p} \tag{24}$$

where <**M**> is an averaged tensor property. The following orientation averaging scheme is performed to obtain the stiffness as the fourth order tensor.

$$\begin{aligned}\langle C \rangle_{ijkl} = {} & B_1(a_{ijkl}) + B_2(a_{ij}\delta_{kl} + a_{kl}\delta_{ij}) \\ & + B_3(a_{ik}\delta_{jl} + a_{il}\delta_{jk} + a_{jl}\delta_{ik} + a_{jk}\delta_{il}) \\ & + B_4(\delta_{ij}\delta_{kl}) + B_5(\delta_{ik}\delta_{jl} + \delta_{il}\delta_{jk})\end{aligned} \tag{25}$$

B_1 through B_5 are invariants which can be evaluated from the properties of the unit cell.

$$B_1 = C_{11} + C_{22} - 2C_{12} - 4C_{66}$$

$$B_2 = C_{12} - C_{23}$$

$$B_3 = C_{66} + \frac{1}{2}(C_{23} - C_{22})$$

$$B_4 = C_{23}$$

$$B_5 = \frac{1}{2}(C_{22} - C_{23}) \tag{26}$$

The fourth order orientation tensors in the eq. (25) are approximated by the hybrid closure. Finally, modulus distribution can be obtained from the inverse of $\langle C \rangle_{ijkl}$ tensor.

3. Experiment

Polystyrene pellets reinforced with 3 vol% (4.5 wt%) carbon fibers were mixed by using a twin-screw extruder (PRISM, UK). The extrusion took place at the temperature of 200°C and the extrudates were cut into pellets. The average fiber diameter was 6.8 μm according to the suppliers.

Tensile specimens were injection-molded by using an injection molding machine (Battenfeld). Dimension and shape of the injection-molded specimens are showed in Fig. 2. The injection pressure was 8 MPa; holding pressure was 7.5 MPa and barrel temperature was 200°C; mold temperature was 60°C and filling time was 1.6 sec; holding time was 5 sec; cooling time was 25 sec.

Thin layers were successively removed from the specimen by using a milling machine (MD-30B, Hann Keun Machinery & Co., Ltd.). During milling, the specimens were held flat by a double-sided adhesive tape.

Many difficulties in applying the layer-removal method to polymers have been reported (Jansen *et al.*, 1999). The most critical problem is the influence of additional stresses which may occur during machining. Thus, it is very important to decide the appropriate milling speed in order not to introduce additional machining stress. To decide an optimal milling speed, injection-molded neat polystyrene spec-

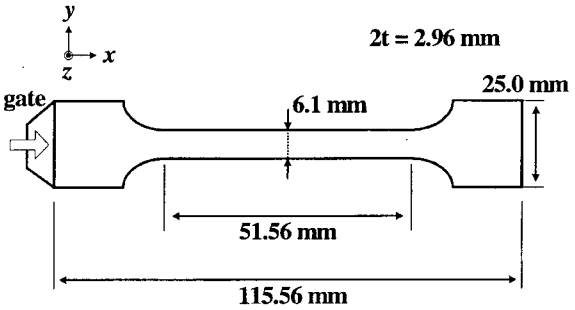

Fig. 2. Dimension of the injection-molded specimen.

imens which were treated for 1 hr at 80°C, i.e., 10°C below the glass transition temperature to remove thermal stresses (Hastenberg *et al.*, 1992) were studied. After successive layer removals at the optimal machining speed, the specimens showed essentially no deflection, which indicates the absence of any stresses introduced by machining. Various milling speeds were tested with the annealed neat polystyrene specimens and 1450 rpm showed the least deflection of all.

The excessive heating caused by mechanical milling can be a drawback in layer-removal of polymeric materials of which the heat conduction is poor. To eliminate the errors due to the machining heat generation and to make the machined surface smoother, cutting oil was used. The specimens before layer removal and the deformed specimen after layer removal are shown in Fig. 3.

After the layer removal was done, the images of the specimens were scanned and the curvature was measured by image processing using a simple geometric principle illustrated in Fig. 4 and the following equation.

$$\rho = \frac{4\sqrt{L_0^2 - L^2}}{L_0^2} \tag{27}$$

where L_0 is the length of the specimen and L is the distance between the two ends of the specimen after layer-removal and ρ is the curvature. The image processing was conducted by using a commercial image analysis tool (Image Pro Plus 4.1, Media Cybernetics®).

The relaxation and creep behavior can occur due to the viscoelastic nature of the polymer. Jansen *et al.* (1999) performed a recovery experiment with a curved strip that was initially stress free. They first pushed the initially curved specimen flat and then measured the time to recover the original curvature of the specimen again after loads were removed. The samples showed almost 96 to 98% recoveries after 10 minutes. Therefore, the curvature was always measured after 10 minutes after layer removal in this experiment.

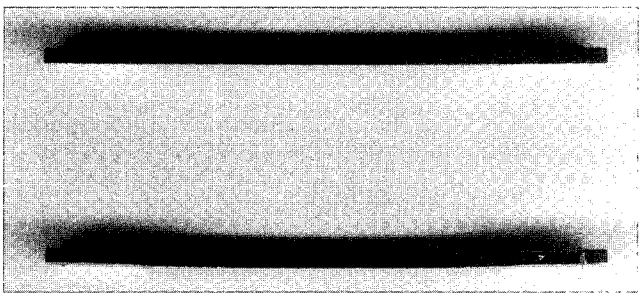

Fig. 3. Specimens before and after layer removal ($z_0 - z_1$=0.24 mm).

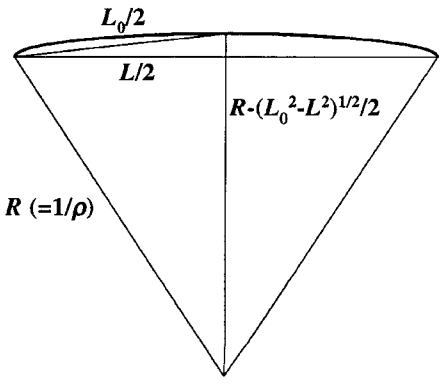

Fig. 4. Determination of the curvature of a deformed plate.

4. Results and discussion

The curvature is defined as positive when the specimen warps concave and as negative when convex after layer removal and the initial curvature is assumed to be zero. The measured curvature data are interpolated by using natural cubic spline, which is a series of third-order polynomial functions between two data points and of which the first and second derivatives are continuous at all points. The curvature data in x-direction with respect to z_1 and the interpolation function are shown in Fig. 5. It can be seen that the curvature continually increases having a negative sign as the removed thickness increases. The curvature in the transverse direction (y-direction) is negligibly small compared with the curvature in the x-direction. From the interpolation function of the curvature, the derivatives and integrals of the fitted curve are obtained.

For the Treuting and Read analysis, Young's modulus and Poisson's ratio need to be determined as constant. They are evaluated by using Halpin-Tsai equation (eq. (14)-(19)) and mixture rule (eq. (20)) with the assumption

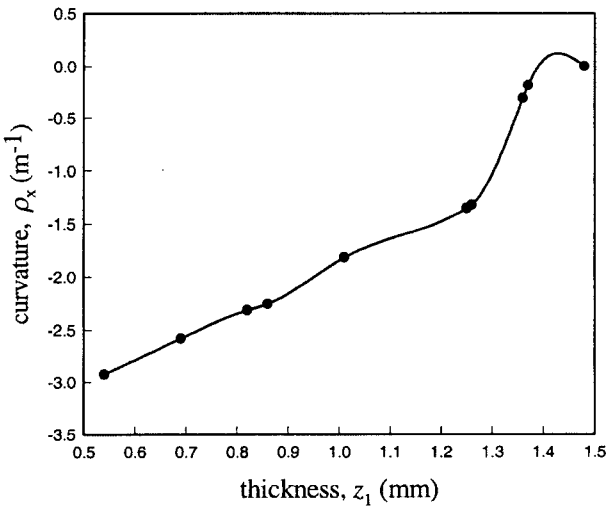

Fig. 5. Measured curvature and fitted curve by natural cubic spline function.

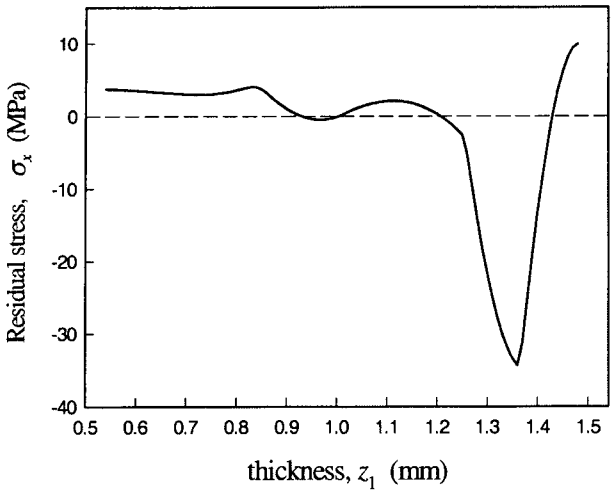

Fig. 6. Residual stress distribution determined from the measured curvature by using the method proposed by Treuting and Read.

of unidirectional fiber orientation. That is, all fibers are assumed to be aligned in the flow direction. Mechanical properties of polystyrene and carbon fibers are known from the suppliers. Moduli of matrix and fiber, E_m and E_f, are 41 MPa and 264 GPa, respectively; Poisson's ratios of matrix and fiber, ν_m and ν_f, are 0.33 and 0.20, respectively. Calculated modulus and Poisson's ration of the composite material are 1.79 GPa and 0.33. They are used in the eq. (4) along with the measured curvature, derivatives of the curvature, and integrals of the curvature to determine residual stress distribution through the thickness. The determined residual stresses are plotted in the Fig. 6. It can be seen that half the cross-section of the specimen can be subdivided into three regions, which are a surface region with tensile stresses, a core region with tensile stresses, and an intermediate region with compressive stresses, although there are some deviations in the intermediate region due to experimental errors. This profile has been proved to be as a typical residual stress distribution of the injection molded materials. The maximum tensile stress at the surface region is determined to be 10 MPa and the maximum compressive stress approximately 34 MPa. These values should be regarded as over-predicted ones because all fibers are assumed to lie in the flow direction while injection molded specimens do not show complete alignment of fibers in the flow direction. The molded samples are likely to have the variation in fiber orientation states with respect to the thickness direction as well as with respect to the plane

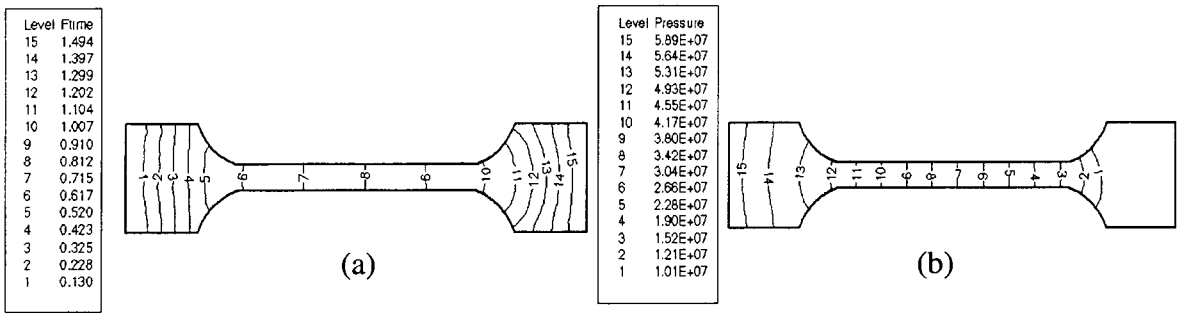

Fig. 7. Numerically predicted (a) flow front advancement and (b) pressure distribution at the end of filling stage of injection molding process.

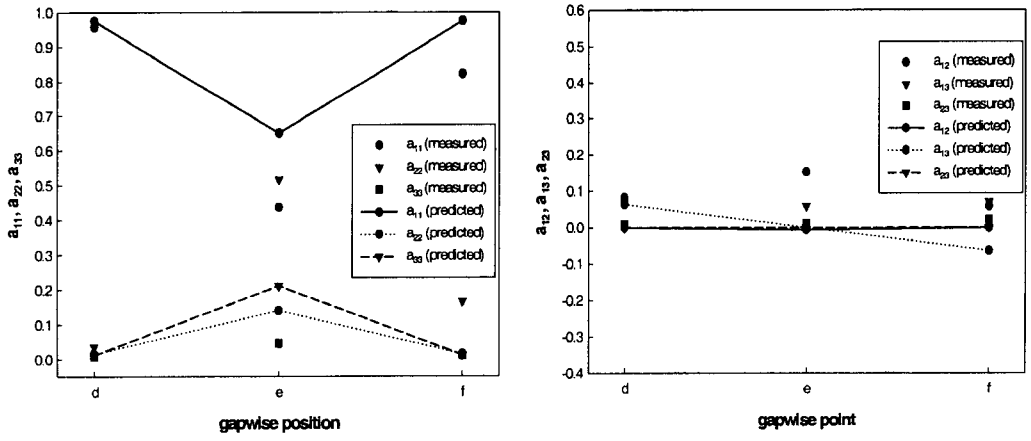

Fig. 8. Measured and predicted fiber orientation tensors across the thickness.

direction. Thus, modulus may vary in the thickness direction according to the corresponding orientation states.

It is previously noted that the residual stress distribution can be determined with the formula proposed by White as long as the modulus distribution is known and the curvature data are obtained by layer-removal. Flow field required for the prediction of fiber orientation is obtained by numerical simulation and some results are shown in Fig. 7. In the previous study by Lee *et al.* (2001), the fiber orientation tensor measured by a confocal microscope showed a good agreement with the numerically predicted fiber orientation tensor. The results are shown in Fig. 8. Therefore, it is quite reasonable to use the predicted Young's modulus distribution calculated from the numerical simulation of injection molding instead of the experimental results. Young's modulus distributions across the thickness calculated by the procedure mentioned above are shown in Fig. 9. The distribution is symmetrical about the center plane of the plate. Measured curvature variation, derivatives of the curvature, integrals of the curvature, and distribution of Young's modulus are used in the eq. (10) to obtain the derivatives of the moment, and they are used in the eq. (9) to determine the distribution of residual stresses across the thickness. The determined stress profile is plotted in Fig. 10.

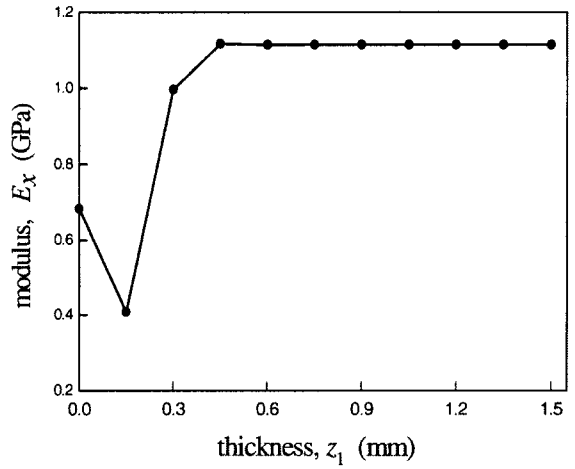

Fig. 9. Calculated Youngs modulus distribution through the thickness.

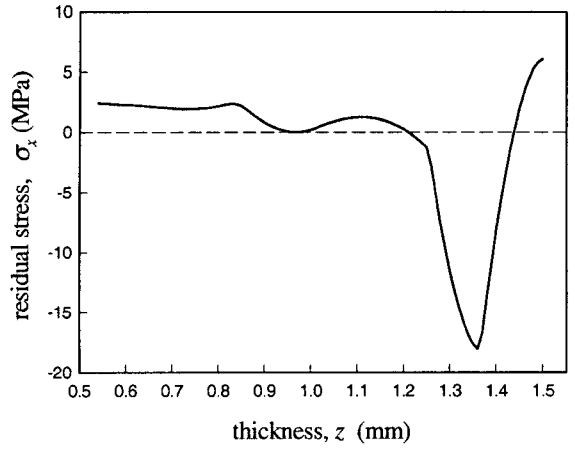

Fig. 10. Residual stress distribution determined from the measured curvature and predicted Young's modulus by using the method proposed by White.

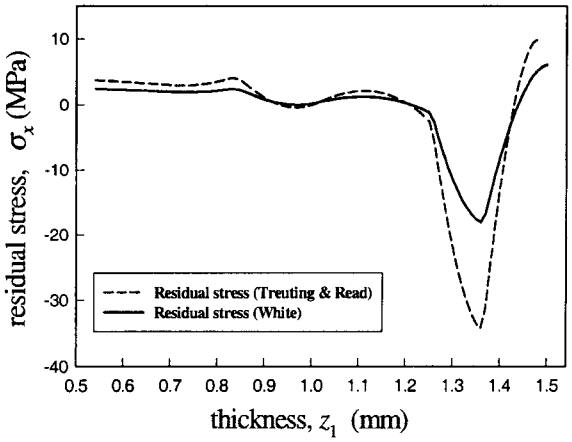

Fig. 11. Comparison between residual stress distributions obtained by White analysis and that by Treuting and Read analysis.

It can be seen that the residual stress distribution shows a similar profile to that by Treuting and Read analysis in Fig. 6, in which there are also a surface region with tensile stresses, a core region with tensile stresses, and an intermediate region with compressive stresses. The maximum tensile stress is determined to be about 6 MPa and the maximum compressive stress to be 18 MPa.

It can be seen in Fig. 11 that there is a difference between the result by White analysis considering Young's modulus distribution and that by Treuting and Read analysis using the uniform modulus. Both of the residual stress distributions have a similar profile, but the magnitude of the maximum stress is somewhat different. Due to difficulties in removing thicker part from the sample the experimental domain is confined only to the two-thirds of half the specimen, where Young's modulus distribution does not change severely so that the modulus remains almost constant as shown in Fig. 8. The residual stress distributions only differ in the magnitude and have resembling results.

5. Conclusions

The residual stress distribution with respect to the thickness of the injection-molded short fiber reinforced composites is determined by the layer-removal method using White analysis in which Young's modulus variation is considered, instead of Treuting and Read analysis in which a uniform modulus distribution is assumed. The curvature changed by upsetting the stress equilibrium is measured

after removal of layers with different thickness and Young's modulus distribution is predicted by numerical simulation of the injection molding process. In general, the residual stress distribution shows tensile stresses at the surface and core regions and compressive stress at the intermediate region, which is well-known as the characteristic residual stress distribution in injection-molded parts. Although White analysis shows a similar result with Treuting and Read analysis and is rather laborious, considering Young's modulus distribution is more appropriate for the short fiber reinforced injection-molded composites that show varying fiber orientation and modulus distributions with respect to the depth.

Acknowledgement

This study was supported by the Korea Science and Engineering Foundation through the Applied Rheology Center (ARC) at Korea University. The authors are grateful for the support.

References

Advani, S.G. and C.L. Tucker III, 1987, The use of tensors to describe and predict fiber orientation in short fiber composites, *J. Rheol.* **31**, 751.

Advani, S.G. and C.L. Tucker III, 1990, Closure approximation for three-dimensional structure tensors, *J. Rheol.* **34**, 367.

Folgar, F. and C.L. Tucker III, 1984, Orientation behavior of fibers in concentrated suspensions, *J. Reinf. Plast. Comp.* **3**, 98.

Halpin, J.C. and J.L. Kardos, 1976, The Halpin-Tsai equations: A review, *Polym. Eng. Sci.* **16**, 344.

Hastenberg, C.H.V., P.C. Wildervanck, A.J.H. Leenen and G.G.J. Schennink, 1992, The measurement of thermal stress distributions along the flow path in injection-molded flat plates, *Polym. Eng. Sci.* **32**, 506.

Jansen, K.M.B., J.J.W. Orij, C.Z. Meijer and D.J. Van Dijk, 1999, Comparison of residual stress prediction and measurements using excimer laser layer removal, *Polym. Eng. Sci.* **39**, 2030.

Lee, S.W., 1997, Study on the prediction of fiber orientation, mechanical properties, and thermal expansion coefficients of injection-molded short fiber composites, MS thesis, Seoul National University.

Lee, S.W. and J.R. Youn, 1999, Characterization of short glass fiber filled polystyrene by fiber orientation and mechanical properties, *Macromolecular Symposia* **148**, 211.

Lee, K.S., S.W. Lee, J.R. Youn, T.J. Kang and K. Chung, 2001, Confocal microscopy measurement of the fiber orientation in short fiber reinforced plastics, *Fibers and Polymers* **2**, 41.

Paterson, M.W.A. and J.R. White, 1989, Layer removal analysis of residual stress II: A new procedure for polymer mouldings with depth-varying Youngs modulus, *J. Mater. Sci.* **24**, 3521.

Treuting, R.G. and W.T. Read Jr., 1951, A mechanical determination of biaxial residual stress in sheet materials, *J. Appl. Phys.* **22**, 130.

White, J.R., 1985, On the layer removal analysis of residual stress I: Polymer mouldings with depth-varying Youngs modulus, *J. Mater. Sci.* **20**, 2377.